Journal of Colloid and Interface Science 424 (2014) 37–43

Contents lists available at ScienceDirect

Journal of Colloid and Interface Science

www.elsevier.com/locate/jcis

Influence of the solvent in the synthesis of zeolitic imidazolate framework-8 (ZIF-8) nanocrystals at room temperature

Eugenia L. Bustamante [a], José L. Fernández [b], Juan M. Zamaro [a,*]

[a] Instituto de Investigaciones en Catálisis y Petroquímica, INCAPE (FIQ, UNL, CONICET), Santiago del Estero 2829, (3000) Santa Fe, Argentina
[b] Programa de Electroquímica Aplicada e Ingeniería Electroquímica, PRELINE (FIQ, UNL), Santiago del Estero 2829, (3000) Santa Fe, Argentina

ARTICLE INFO

Article history:
Received 3 January 2014
Accepted 5 March 2014
Available online 12 March 2014

Keywords:
Metal–organic framework
ZIF-8
Porous nanomaterial
Solvent effect
Crystallization

ABSTRACT

The effect of the solvent on the synthesis process and on the nanocrystal characteristics of the zeolitic imidazolate framework-8 (ZIF-8) was investigated. A synthesis protocol at room temperature employing a series of aliphatic alcohols, water, dimethylformamide and acetone was employed. The results show that the solvent modifies the evolution of the reaction, altering the crystallization rates and nanocrystal sizes. Its hydrogen bond donation ability is the main factor that governs this effect. More precisely, the solvent modulates the formation of ZIF-8 nanocrystals with sizes in the range between 15 and 42 nm. When synthesized in alcohol and acetone, these nanocrystals form globular aggregates with sizes between 130 and 420 nm. In contrast, under the same synthesis conditions, when using water or dimethylformamide the ZIF phase is not developed. In alcohols other than methanol, the crystals develop pill-shaped morphologies with poorly defined facets. Moreover, a markedly fast growing kinetics is verified in these alcohols, leading to an ultra-fast crystallization of ZIF-8 in about 60 s. These findings provide new information about the role of the solvent in the synthesis process of nanoZIF-8, which can be useful for controlling the crystallization rates and nanocrystal sizes of this material.

Introduction

Zeolitic imidazolate frameworks (ZIFs) are a subclass of metal organic frameworks (MOFs) with zeolite-type topology and outstanding thermal and chemical stability [1]. ZIF-8, one of the most widely studied ZIFs, was originally synthesized as microcrystals by Yagui and co-workers using dimethylformamide (DMF) [2]. This MOF has **sod** (sodalite-type) topology, with pore size of 11.6 Å and window openings of 3.4 Å even though its structure is flexible and allows the entry of larger molecules than this window size [3]. In general, solvothermal methods using amide-type solvents have been developed for the synthesis of ZIFs [1]. The fabrication of these microporous materials under the shape of nanosized crystals (nano-MOFs) could be highly valuable for the development of new functional and nanotechnological applications [4]. More specifically, nano-MOFs could be advantageous in catalysis and adsorption processes due to the decrease in diffusive resistances [5] as well as in controlled drug release applications [6]. Moreover, they can be used as a new type of filling in mixed-matrix membranes for gas separation [7] and for the preparation of supported membranes by secondary synthesis methods [8].

In particular, ZIF-8 has been synthesized under the shape of nanocrystals by methods involving simple mixing of the components at room temperature in methanol [9,10]. More recently, nanocrystals of this material have also been obtained in water [11]. However, the regulation of the ZIF-8 crystal morphology and crystal size distribution at the nanoscale level is still a challenge. The control of crystal size distribution has been achieved by means of different strategies such as the adjustment of the reagent ratios [12], the incorporation of additives (i.e. trialkylamine) [13], cetyltrimethylammonium bromide [14], small amounts of the polyelectrolyte poly-diallyldimethylammonium chloride [15], formate [16] and ancillary ligands with different chemical functionalities [17]. The sources of Zn have also been modified, leading to the formation of ZIF-8 phases coexisting with ZnO nanoneedles [18]. Besides the above protocols, other non-conventional methods have also been used to regulate the size of ZIF-8 nanocrystals, such as sonocrystallization [19], microwave irradiation [20], using a micromixer [21] or by ionothermal microwave-assisted synthesis [22]. In all the above mentioned cases, ZIF-8 was synthesized using only three solvents: DMF, water and methanol. In general, in the design of synthetic methods for MOF fabrication, less attention has been given to this parameter and a small number of solvents have been used [23]. However, the synthesis medium should play an important role in the coordination chemistry of supramolecular

* Corresponding author. Fax: +55 0342 4536861.
E-mail address: zamaro@fiq.unl.edu.ar (J.M. Zamaro).

http://dx.doi.org/10.1016/j.jcis.2014.03.014
0021-9797/

systems [24]. In this context, this study performs a systematic exploration of the influence of the solvent on the formation rate and nanocrystal characteristics of the archetypical MOF ZIF-8, using a synthesis protocol at room temperature.

Experimental

Synthesis methodology

A synthesis protocol reported by Cravillon et al. [9] was taken as reference. In this work, $Zn(NO_3)\cdot 6H_2O$ (Aldrich 99.0%), 2-methylimidazole (Aldrich 99.0%) and the selected solvent were mixed in molar proportions of 1:8:700, respectively. Methanol (Cicarelli, 99.8%), ethanol (Cicarelli, 99.5%), n-propanol (Dorwil, 99.5%), 2-propanol (Cicarelli, 99.5%), n-butanol (Cicarelli, 99.4%), 2-butanol (Merck, 99.5%), n-octanol (Merck, >99%), dimethylformamide (DMF, Aldrich, 99.0%), acetone (Cicarelli, 99.5%), and distilled water were the different solvents employed. First, $Zn(NO_3)\cdot 6H_2O$ and 2-methylimidazole were dissolved separately in equal amounts of the respective solvent. Then, the first solution was rapidly added onto the second one under agitation (350 rpm) at room temperature. Stirring was continued for time periods ranging from 1 to 480 min and the solids thus formed were recovered by centrifugation at 7000 rpm for 5 min. Once separated, they were re-suspended in methanol in order to be washed and centrifuged. This operation was repeated twice and finally the materials were dried overnight in an oven at 70 °C.

Characterization of synthesized materials

X-ray diffraction (XRD) was performed with a Shimadzu XD-D1 instrument by scanning the 2θ angle at 2° min^{-1} between 5° and 50° using Cu Kα radiation (λ = 1.5418 Å, 30 kV, 40 mA). The relative crystallinity was calculated using the integrated peak areas of the diffraction peaks at 2θ = 7.4°, 10.4°, 12.7° and 18.06°, and considering 100% crystallinity for the sample synthesized in methanol after 120 min. The mean crystallite size (t) was estimated using the Scherrer equation: $t = 0.9\ \lambda/(B\cos\theta)$, where $B^2 = B^2_{\text{sample}} - B^2_{\text{standard}}$. The intrinsic broadening of the diffraction signals (B_{standard}) was estimated using a standard Si single crystal [25] and the validity of this equation was confirmed by verifying the expected linear relationship between $\cos(\theta)$ and B^{-1} for the four peaks considered for each sample. Scanning electron microscopy (SEM) was performed on glass-supported samples with a JEOL JSM-35C operated at 20 kV. Thermogravimetric analysis (TGA) was conducted with a Shimadzu TGA-51 instrument from 25 °C to 1000 °C at 10 °C min^{-1} in N_2 flow (50 mL min^{-1}, STP). Analysis by atomic force microscopy (AFM) was carried out in the non-contact mode with an Agilent 5400 microscope on glass-supported dispersed samples. The turbidity evolution of the synthesis medium during the reaction was followed with a LaMotte 2020e nephelometer furnished with a tungsten lamp (2300 °C) and a photodiode detector located at 90°. The apparent pH was monitored with an Altronix pH-meter and a BOECO BA 2S electrode calibrated between measurements. FTIR spectra were taken on powder samples supported in KBr pellets with a Shimadzu 8101 M Prestige-21 instrument equipped with a high sensitivity DLATGS detector, from 400 to 4000 cm^{-1} recording 40 scans with a 2 cm^{-1} resolution.

Results and discussion

Synthesis of ZIF-8 nanocrystals in aliphatic alcohols

In order to gradually vary the physicochemical properties of the reaction medium, a series of individual syntheses was conducted using a sequence of straight and branched aliphatic alcohols as solvents. The molar ratios of the reagents and other synthesis conditions such as temperature, stirring power and reaction time (120 min) were kept constant. Under these conditions, all the solids obtained with the different alcohols were pure and well-developed phases of ZIF-8 (Fig. 1) [2]. This is the first report of the synthesis of ZIF-8 in solvents different from methanol, DMF or water. However, differences in the relative crystallinity and crystallite size were noticed, as shown in Table 1. The materials obtained in methanol and n-octanol showed the highest crystallinity and crystallite size while those obtained in 2-butanol had the lowest values. Even though in all cases the crystallites presented nanometric sizes, the SEM images (Figs. 2 and S1) showed that they were aggregated as globular particles of varying dimensions (Table 1). The variable aggregation level could be associated with the ability of the different solvents to disperse the nanocrystals formed during synthesis. Moreover, the efficiency of the synthesis in a zinc basis appears to be slightly lower for methanol and ethanol, while for other alcohols it was around 40–50% (Table S1). Although a precise determination of the primary crystal sizes was not possible from the SEM micrographs, it can be observed that the estimated crystal sizes are comparable with those calculated by XRD. Furthermore, the edges of the crystals looked rounded, probably because the crystallization proceeded quickly under vigorous stirring.

The solvent can exert thermodynamic and kinetic effects in the assembly of MOFs and the ways in which this occurs can be thus summarized [24]: (i) solvent as ligand; (ii) solvent as guest; (iii) solvent as both ligand and guest (iv) solvent as structure directing agent (SDA). Moreover, it has been found that for a given MOF these effects may be modified by the addition of different aromatic molecules to the synthesis mixture [26]. In the case of ZIFs structures Park et al. [2] postulated that such frameworks are not only produced by an appropriate functionalization of the linker, but also by a SDA effect induced by an amide-type solvent. Similarly, Tian et al. [27] noted that some organic solvents play a key role as SDA or primary template agents in the synthesis of imidazolates with zeolitic topologies. The primary template effect occurs when

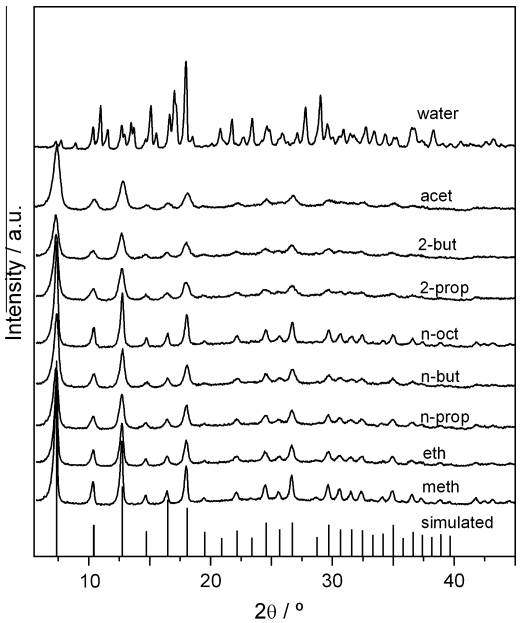

Fig. 1. XRD patterns of the materials obtained after 120 min employing different aliphatic alcohols, acetone and water. Theoretical ZIF-8 pattern was simulated from CCDC archive (602538).

Table 1
Structural properties of the obtained ZIF-8 nanocrystals, α parameter of the solvents and the relative rates of ZIF-8 formation.

Solvent	Relative crystallinity[a]	Crystallite size at 120 min/nm[b]	Crystallite size at 60 s/nm[b]	Aggregate size at 120 min/nm[c]	α [33]	r^0_{rel} [d]
Methanol	1.00	42.1	–	134 ± 15	0.98	1.0
Ethanol	0.82	31.3	16.6	342 ± 56	0.86	14.6
n-Propanol	0.80	22.5	16.7	212 ± 63	0.84	14.1
2-Propanol	0.81	19.7	20.1	421 ± 103	0.76	18.2
n-Butanol	0.89	24.7	22.8	324 ± 77	0.84	12.3
2-Butanol	0.63	17.8	18.1	372 ± 122	0.69	15.3
n-Octanol	0.97	35.2	27.7	413 ± 94	0.77	–
Acetone	0.93	14.8	–	–	0.08	32.5
Water	–	–	–	–	1.17	–
DMF	–	–	–	–	0.00	0.6

[a] Estimated by integrating the main XRD signals and considering 100% crystallinity for the sample synthesized in methanol.
[b] Estimated from Scherrefs equation: $t = 0.9\ \lambda/B\cos\theta$; $B^2 = B^2_{sample} - B^2_{standard}$ in which B is the full width at half maximum (FWHM).
[c] Estimated from SEM pictures.
[d] r^0_{rel} is the ratio of initial turbidity (15 s) of the reaction mixture in methanol and the initial turbidity of the reaction mixture in the respective solvent.

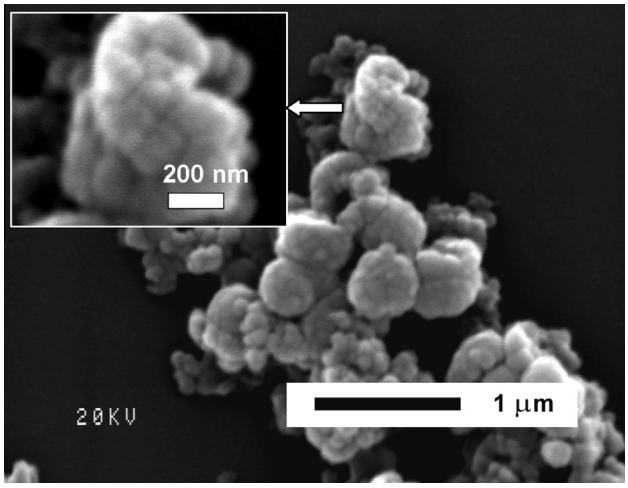

Fig. 2. SEM image of the solid obtained after 120 min in n-octanol. The inset is a zoom in a region of 0.9 × 0.7 μm.

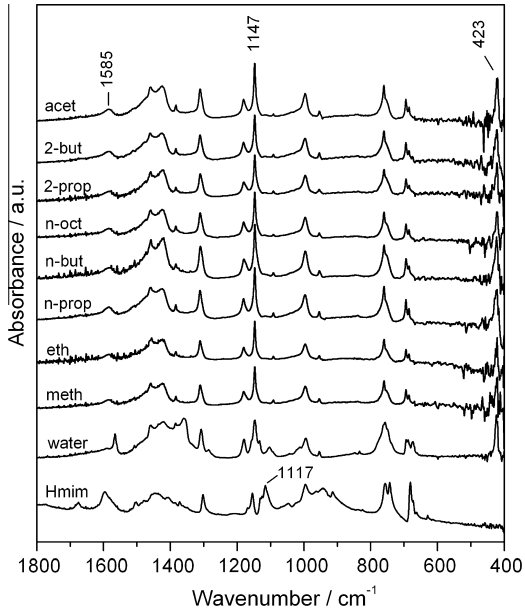

Fig. 3. FTIR spectra of the solids obtained after 120 min synthesis in the alcohols series; acetone and water. Spectrum of 2-methylimidazole (Hmim) is also shown.

the solvent acts as a mold of the structure and is included in the framework by non-covalent interactions [28]. Meanwhile, a SDA effect takes place when the formation of a MOF or the increase in its growth rate is favored by the solvent [29]. From the above discussion and in view of our results in which almost identical ZIF-8 phases can be obtained in such different alcohols, with differences in crystallinity, crystallite size, extent of aggregation, and formation rate (shown later) it can be concluded that the solvent is probably involved as a SDA.

Furthermore, the grain boundaries and sizes of the nanocrystals were analyzed by AFM using topographic and phase-contrast images as those shown in Fig. S2. These AFM images show nanocrystals with apparently rounded edges and, in some cases, slightly faceted shapes, whose sizes vary between 20 and 40 nm. This confirms the crystallite characteristics previously estimated by XRD and SEM.

The FTIR spectra of the obtained materials (Fig. 3) confirm that the chemical bond structure corresponds to that reported for ZIF-8 [2]. Fig. S3 shows the main bond connectivity in the motif of the ZIF-8 structure and in the 2-methylimidazole, which are associated with the main FTIR bands observed. Imidazole derivatives such as 2-methylimidazole possess a typical IR spectrum with a broad absorption band in the 2250–3300 cm^{-1} frequency region due to vibrations of the hydrogen bonds established between the pyrrole group and the pyridinic nitrogen [30]. This absorption band and the associated signal at 1850 cm^{-1} are absent in the IR spectra of materials obtained in alcohols and acetone (Fig. S4), which indicates the formation of imidazolates. The signal around 1585 cm^{-1} is due to the stretching mode of C=N, while that observed in the region between 1350 and 1500 cm^{-1} is associated with the vibration of the ring [31]. A shift of the CH bending signal from 1117 cm^{-1} to 1147 cm^{-1} was observed (Fig. 3), which can be assigned to the transformation of imidazole to imidazolate [30]. Bands in the region below 800 cm^{-1} are usually caused by out-of-plane bending of the ring [31] and the peak at 423 cm^{-1} is due to the vibration mode of Zn—N [32]. The presence of this latter signal in all samples synthesized in alcohols indicates that Zn cations are connected to nitrogen atoms of the methylimidazole groups forming the imidazolate (Fig. S3).

Interactions of the solvents during nanocrystal formation

The syntheses of ZIF-8 nanocrystals were also conducted in water, DMF and acetone, using the same synthesis conditions employed for the syntheses in the alcohols. It should be noted that ZIF-8 crystals were previously obtained in DMF and water [2,11], but these syntheses were conducted using other molar compositions of reactants and/or temperatures. After mixing the reactants

in water, the formation of a white suspension was observed but the XRD pattern of the solid obtained did not match the ZIF-8 structure but seemed to correspond to an imidazolate with denser structure (Fig. 1), which is also supported by the FTIR spectrum of this sample (Fig. 3).

On the other hand when using DMF, turbidity was not visually observed even after 120 min, although the presence of nano-particles was detected by the Tyndall effect when illuminating the suspension with a laser (Fig. S5). This DMF-based mixture was left to rest for 6 months and, after this period, no changes were noticed; furthermore, it was not possible to isolate the solids even centrifuging at 15,000 rpm. This low solid content was confirmed by studies of turbidity as shown below. Then, it can be considered that the extent of ZIF-8 formation in this solvent, compared with that of the other solvents, was negligible. Meanwhile, when using acetone a white precipitate was rapidly produced which corresponded to a pure phase of ZIF-8 (Figs. 1 and 3) with the smallest crystallite size (Table 1).

It should be noted that the syntheses in water and DMF that we report in this work did not lead to previously reported results because other conditions were used, which surely are not the optimum conditions to obtain the material in these two solvents. In particular, we tried to keep constant the molar ratio of the reactants at the same value that was used with the alcohols. In this way, we made sure that the observed effects were only related to the properties of the solvents. Our experiments show a remarkable effect of the solvent in the reaction between Zn^{2+} and 2-methylimidazole, which can lead to the formation of both an undesired phase (in water) and developed phases of ZIF-8 with different sizes and degree of crystal aggregation (in alcohols and acetone) under the same synthesis conditions. It could also lead to practically inhibit the phase evolution (in DMF). All the solvents used (protic and aprotic) were polar and had different capabilities to dissolve and to solvate Zn^{2+}, NO_3^- ions and the organic ligand because of their different dielectric constants, dipole moment and van der Waals volume [24]. However, the studied solvents had other properties that would modulate the assembly between the organic ligand and the metal center in the formation process of ZIF-8. In this sense, a series of parameters that characterize specific molecular interactions for different types of solvents, called solvatochromic parameters, have been defined [33]. They were obtained with appropriate solutes so that the contribution of each type of molecular interaction can be discriminated and differs from other macroscopic properties such as the permittivity (ε). Among these, parameters ET-30 (defined as a polarity index), α (which characterizes the ability of hydrogen bond donation, or HBD), and β (which represents the capacity to accept and stabilize protons) are the most relevant ones in this analysis.

It can be seen (Table S1) that while DMF has an ET-30 value comparable to that of the alcohols, in this solvent no evolution of the ZIF-8 was verified. Besides, water (where no ZIF-8 phase developed) has the highest ET-30 value of the series. This may suggest that an optimum value of this parameter is needed. However, as acetone has a lower ET-30 value than DMF, the connection between the ZIF-8 formation and the ET-30 parameter is discarded. When analyzing β (Table S1), it can be seen that all the solvents studied have the capacity to accept and stabilize protons, but neither of them shows a clear correlation between the ZIF-8 evolution or crystal characteristics with this parameter.

By contrast, when the α parameter of the solvents is analyzed (Table 1), a clear correspondence with the results can be observed. For DMF, which is an aprotic solvent that has a non-polarized hydrogen atom, the value of α is zero. Meanwhile, water has the highest α value, while acetone, despite being aprotic, has a certain HBD capacity. The apparent correlation of the results obtained in this work with the HBD capacity of the solvent suggests that this parameter may affect the evolution of ZIF-8. Bertrán et al. [34] reported that the formation of a Zn imidazolate initially involves the coordination of the metal atom with the electron-deficient pyridinic nitrogen of the imidazole group. This coordination polarizes the proton of the pyrimidine group, then allowing another Zn^{2+} cation to coordinate with the other nitrogen of the imidazole. In a solvent with polar characteristics and capable of generating hydrogen bonds, a greater lability of the pyrimidinic proton could be induced facilitating the evolution of the reaction (see Fig. S3). Fig. 4 shows the relationship between the crystallite size and the α values, which verifies a good correspondence that only moves away from the apparent trend in the case of n-octanol. However, as this last alcohol has a long carbon chain, other factors that are simultaneously involved (such as the ion solvation capacity and dispersion of the formed crystals) may have a greater influence in this case.

The relationship between the progress in ZIF-8 formation and the solvent interaction agrees with the results found by Moh et al. [35], who monitored by in situ AFM the molecular assembly of ZIF-8 during its synthesis in methanol. They concluded that the formation of the ZIF-8 is dependent on the presence of non-framework species (solvent) that provide interactions that stabilize the pores of the network during the crystal growth. The interaction between solvent and framework was also suggested from crystallographic data reported for ZIF-8 [2], which indicated the presence of solvent molecules near the hydrogen atoms of methylimidazolate groups.

Evolution of the ZIF-8 nanocrystal formation

The rates of the formation of the solids in the series of alcohols, except for methanol, were very high and turbidity was immediately observed when the reagents were mixed. The turbidity, measured as the intensity of the scattered light, depends on the particle concentration, size, shape, and aggregation [36]. The turbidimetric curves (Fig. 5a) show that within the first 5 min the rate of solid formation was high and similar for all the alcohols, except for methanol. For the latter, a plateau for about 90 s is observed which indicates an induction period [9]. Then the turbidity raised due to an increase in the number of particles (nucleation) and in the particle size (growing), as already proposed for these synthesis conditions [10]. After about 20 min, the turbidity change became smaller, which is compatible with a low crystal growth rate caused by a capping effect of the ligand on the surface of the crystals [9,16]. In contrast, the evolution of the solids in the other alcohols showed a fast initial rate, which decelerated from approximately

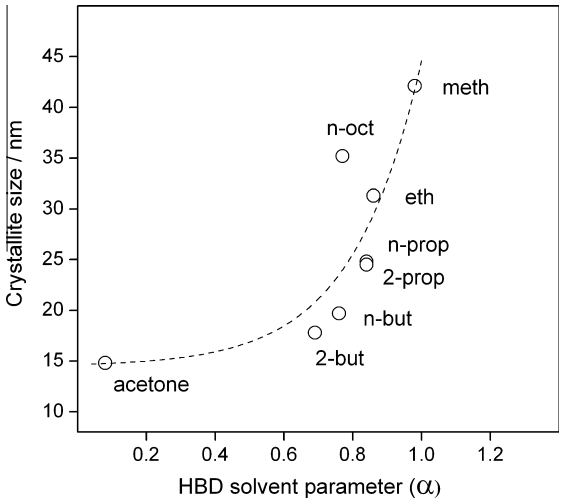

Fig. 4. Plot of ZIF-8 crystallite size after 120 min synthesis vs the hydrogen bond donation parameter (α) of the solvent.

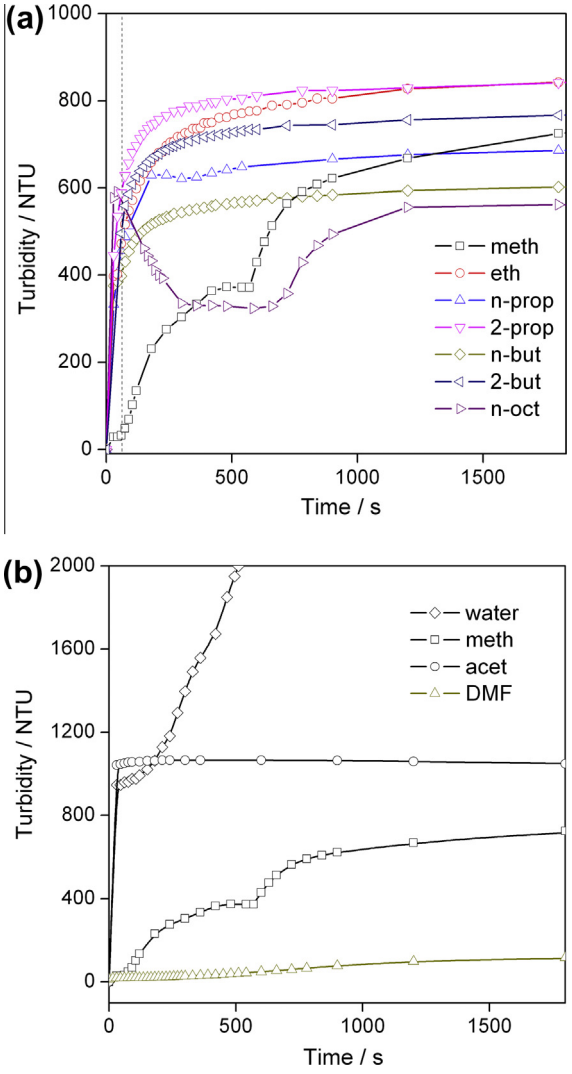

Fig. 5. Turbidimetric curves during syntheses in different solvents: (a) alcohols; (b) non alcohols.

60 s (dotted line). As shown below (Ultrafast synthesis of ZIF-8 nanocrystals), this evolution corresponds to a crystallization process. The maximum observed for n-octanol was due to the formation of large aggregates, which were later partially redispersed. The amount of solid produced in DMF was very low and remained virtually unchanged throughout the analyzed period (Fig. 5b). Meanwhile, the curve corresponding to the synthesis in acetone shows a faster increase at the beginning of the reaction, which reflects the rapid nucleation and crystal growth in this solvent, in agreement with the XRD results.

On the other hand, the proton concentration in the different solvents was followed and measured as an apparent pH. A sharp initial drop was observed in all synthesis mixtures (Fig. S6) which can be assigned to the acidity introduced by the zinc solution and the ligand deprotonation during the reaction. The drop of the apparent pH (ΔpH) in all mixtures ranged between 2.1 and 2.7 (Fig. S6) and a clear correlation between the extent and/or the rate of crystallization and the acido-base properties cannot be established. This evidence reinforces the hypothesis that the formation of ZIF-8 is influenced by interaction effects of the solvent rather than by the acidity-basicity of the medium. This can also be related to the studies of formation of polymeric imidazolates in solid phase [30]. In this sense, it was observed that the imidazole does not react with very basic oxides, indicating that the first step of the reaction is not the removal of pyrrolic hydrogen but the complexation of the pyridinic nitrogen by the cation, with the subsequent release of the proton. This process is further enhanced by binding the expelled proton to a basic entity, such as imidazole, nitrate or the solvent.

Ultrafast synthesis of ZIF-8 nanocrystals

Given the high rates of solid formation using alcohols different from methanol, the solids produced after 60 s were collected and analyzed by XRD. Their diffractograms surprisingly exhibited signals of well-evolved and pure ZIF-8 phases (Fig. 6), indicating that the evolution of solids at the initial stages is due to a rapid crystallization process. To our knowledge, these are the highest crystallization rates reported so far for the various synthetic protocols for obtaining this MOF [2,9–22]. The efficiency of the synthesis was somewhat lower compared to that produced at 120 min but remains around 20–30% (Table S1). The crystallite sizes of the obtained solids were generally slightly lower than those found at 120 min, and in some cases (for example in 2-propanol and 2-butanol) practically remained constant (Table 1). These trends are in agreement with the low slope of the turbidimetric curves beyond 60 s (dotted line in Fig. 5a). Moreover, the processing of XRD signals yield crystallinity values practically identical to those of the materials obtained after 120 min. The evolution of the nanocrystal size is exemplified with the solids obtained in n-propanol, which in the course of 1 h increased their crystallite size only about 3.3 nm (Fig. S7). Since the fast crystallization is reflected by the change in turbidity at the first moments, a relative initial crystallization rate (r^0_{rel}) can be estimated relating the turbidity after 60 s for each alcohol (except for n-octanol in which agglomerates were produced) with respect to that of methanol (Table 1). It can be observed that the growth rate in any alcohol other than methanol was an order of magnitude greater, while it was very low in DMF. The FTIR spectra of these solids (Fig. S8) correspond to a pure phase of ZIF-8 and no signals from minority phases can be detected (such as unreacted 2-methylimidazole), confirming that the formation of the ZIF-8 structure proceeded completely.

In the topographic AFM image of the sample synthesized at 60 s in n-propanol (Fig. 7a), rounded edges can be observed, similar to

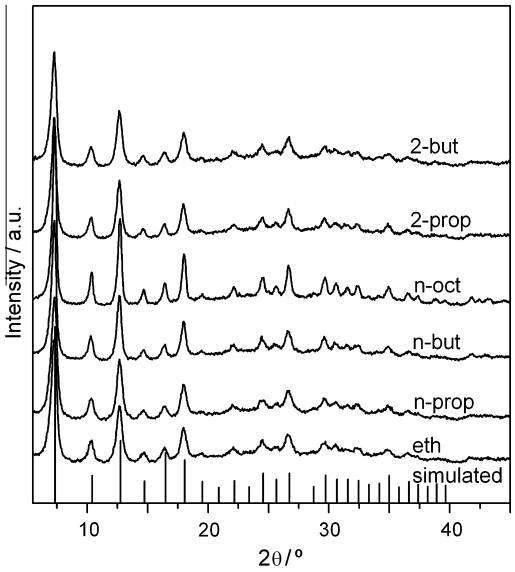

Fig. 6. XRD patterns of the materials synthesized at 60 s employing alcohols different from methanol.

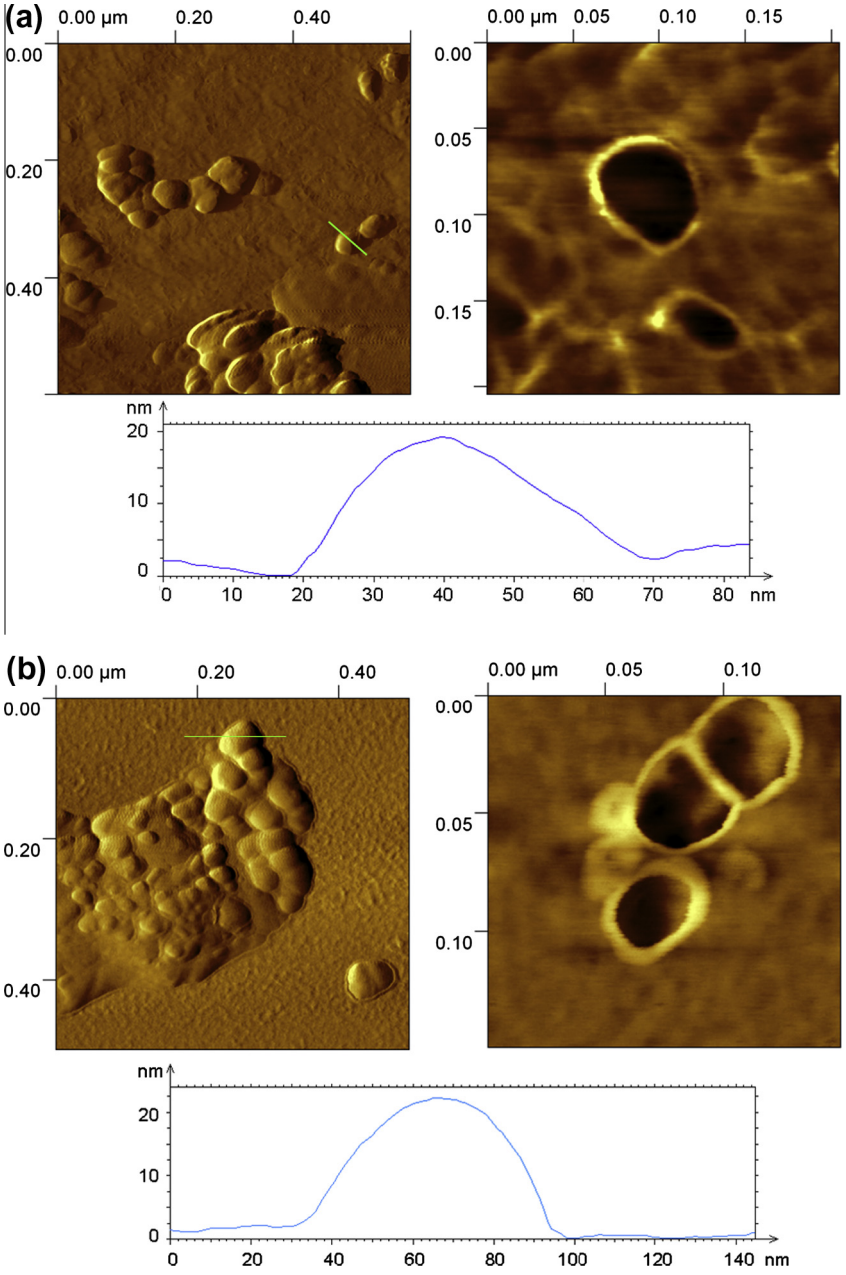

Fig. 7. AFM images (up) and topographic profiles (down) of ZIF-8 nanocrystals synthesized in n-propanol at different times: (a) 60 s; (b) 480 min.

those seen at longer times (Fig. S2). The topographic profile indicates a high aspect ratio of the crystals, with a height of about 17 nm in agreement with the estimations made by XRD. The sample synthesized at 480 min (Fig. 7b) slightly increased its crystal size to about 22 nm, while keeping the flattened profile with rounded edges. Furthermore, all the nanocrystals obtained at 60 s showed a thermal stability up to ~400 °C (Fig. S9), which is comparable to that verified on materials obtained after 120 min and on other reported ZIF-8 nanocrystals [9,12,13,19]. In the TGA profiles of the activated crystals, the small mass loss up to 300 °C (<3%) may be due to the release of water adsorbed at the crystal surface and residuary solvent inside the pores. Subsequently, near 400 °C, the sharp mass loss is due to the collapse of the framework with release of organic material. The differences in the temperatures at which this occurs may be linked to variations in the packing between the aggregated nanocrystals, which generate different mass transfer resistances to remove the degradation products.

Conclusions

ZIF-8 nanocrystals were synthesized at room temperature in solvents other than those already reported for the synthesis of this MOF. More precisely, a series of aliphatic alcohols and acetone were employed as solvents. These syntheses allowed obtaining pill-like nanocrystals having rounded edges, with variable relative crystallinity, crystallite sizes and aggregation. In contrast when water was used under the same synthesis conditions, the ZIF-8 phase was not obtained whereas in DMF the extent of ZIF-8 formation was very small. These findings show a remarkable effect exerted by the solvent in the reaction between the Zn^{2+} and 2-methylimidazole, and suggest that it plays a role as a secondary structuring agent (SDA) modulating and guiding the formation of the ZIF-8 phase.

The progress of the reaction seems to be influenced by molecular interactions between the reagents and the solvent with hydro-

gen bond donation (HBD) ability, which probably increases the polarization of the pyrimidinic hydrogen, facilitating its deprotonation and subsequently its coordination with Zn^{2+} to follow the reaction. The crystallization rates in non-methanol alcohols were higher than those reported for methanol [9,10], and allowed the ultra fast synthesis (60 s) of nanocrystalline ZIF-8 (16–28 nm) which maintained their structural integrity up to about 400 °C. These results demonstrate the importance of the solvent in the crystallization kinetics and evolution of ZIF-8 nanocrystals.

Acknowledgments

The authors wish to acknowledge the financial support received from Consejo Nacional de Investigaciones Científicas y Técnicas (CONICET), Agencia Nacional de Promoción Científica y Tecnológica (ANPCyT) and Universidad Nacional del Litoral (UNL). Thanks are also given to Elsa Grimaldi for the English language editing.

Appendix A. Supplementary material

Supplementary data associated with this article can be found, in the online version, at http://dx.doi.org/10.1016/j.jcis.2014.03.014.

References

[1] A. Phan, C.J. Doonan, F.J. Uribe-Romo, C.B. Knobler, M. O'Keeffe, O.M. Yaghi, Acc. Chem. Res. 43 (2010) 58–67.
[2] K.S. Park, Z. Ni, A.P. Coté, J.Y. Choi, R. Huang, F.J. Uribe-Romo, H.K. Chae, M. ÓKeeffe, O.M. Yagui, PNAS 103 (2006) 10186–10191.
[3] D. Fairen-Jimenez, S.A. Moggach, M.T. Wharmby, P.A. Wright, S. Parsons, T. Düren, J. Am. Chem. Soc. 133 (2011) 8900–8902.
[4] L. Tosheva, V.P. Valtchev, Chem. Mater. 17 (2005) 2494–2513.
[5] K. Li, D.H. Olson, J. Seidel, T.J. Emge, H. Gong, H.Z.J. Li, J. Am. Chem. Soc. 131 (2009) 10368–10369.
[6] C.-Y. Sun, C. Qin, X.-L. Wang, G.-S. Yang, K.-Z. Shao, Y.-Q. Lan, Z.-M. Su, P. Huang, C.-G. Wang, E.-B. Wang, Dalton Trans. 41 (2012) 6906–6909.
[7] B. Seoane, J.M. Zamaro, C. Tellez, J. Coronas, RSC Adv. 1 (2011) 917–922.
[8] S.R. Venna, M.A. Carreon, J. Am. Chem. Soc. 132 (2010) 76–78.
[9] J. Cravillon, S. Munzer, S-J. Lohmeier, A. Feldhoff, K. Huber, M. Wiebcke, Chem. Mater. 21 (2009) 1410–1412.
[10] S.R. Venna, J.B. Jasinski, M.A. Carreon, J. Am. Chem. Soc. 132 (2010) 18030–18033.
[11] Y. Pan, Y. Liu, G. Zeng, L. Zhao, Z. Lai, Chem. Commun. 47 (2011) 2071–2073.
[12] S. Tanaka, K. Kida, M. Okita, Y. Ito, Y. Miyake, Chem. Lett. 41 (2012) 1337–1339.
[13] A.F. Gross, E. Sherman, J.J. Vajo, Dalton Trans. 41 (2012) 5458–5460.
[14] Y. Pan, D. Heryadi, F. Zhou, L. Zhao, G. Lestari, H. Su, Z. Lai, Cryst. Eng. Commun. 13 (2011) 6937–6940.
[15] S.K. Nune, P.K. Thallapally, A. Dohnalkova, C.M. Wang, J. Liu, G.J. Exarhos, Chem. Commun. 46 (2010) 4878–4880.
[16] M. McCarthy, V. Varela-Guerrero, G.V. Barnett, H.-K. Jeong, Langmuir 26 (18) (2010) 14636–14641.
[17] J. Cravillon, R. Nayuk, S. Springer, A. Feldhoff, K. Huber, M. Wiebcke, Chem. Mater. 23 (2011) 2130–2141.
[18] M. Zhu, S. Venna, J.B. Jasinski, M.A. Carreon, Chem. Mater. 23 (2011) 3590–3592.
[19] B. Seoane, J.M. Zamaro, C. Tellez, J. Coronas, Crys. Eng. Commun. 14 (2012) 3103–3107.
[20] Q. Bao, Y. Lou, T. Xing, J. Chen, Inorg. Chem. Commun. 37 (2013) 170–173.
[21] D. Yamamoto, T. Maki, S. Watanabe, H. Tanaka, M.T. Miyahara, K. Mae, Chem. Eng. J. 227 (2013) 145–150.
[22] L. Yang, H. Lu, Chin. J. Chem. 30–5 (2012) 1040–1044.
[23] G. Férey, Chem. Soc. Rev. 37 (2008) 191–214.
[24] C.-P. Li, M. Du, Chem. Commun. 47 (2011) 5958–5972.
[25] Elements of X-ray diffraction, second Ed., B.D. Cullity Ed., USA, 1978.
[26] M.C. Bernini, N. Snejko, E. Gutierrez-Puebla, E. Brusau, G. Narda, M.A. Monge, Inorg. Chem. 50 (2011) 5958–5968.
[27] Y.-Q. Tian, Y.-M. Zhao, Z.-X. Chen, G.-N. Zhang, L.-H. Weng, D.-Y. Zhao, Chem. Eur. J. 13 (2007) 4146–4154.
[28] D. Tanaka, S. Kitagawa, Chem. Mater. 20 (2008) 922–931.
[29] S.R. Bajpe, C.E. Kirschhock, A. Aerts, E. Breynaert, G. Absillis, T.N. Parac-Vogt, L. Giebeler, J.A. Martens, Chem. Eur. J. 16 (2010) 3926–3932.
[30] J.F. Fernández-Bertrán, M.P. Hernández, E. Reguera, H. Y-Madeira, J. Rodriguez, A. Paneque, J.C. Llopiz, J. Phys. Chem. Solids 67 (2006) 1612–1617.
[31] J. Yao, R. Chen, K. Wang, H. Wang, Micropor. Mesopor. Mater. 165 (2013) 200–204.
[32] Y. Hu, H. Kazemian, S. Rohani, Y. Huang, Y. Song, Chem. Commun. 47 (2011) 12694–12696.
[33] Y. Marcus, Chem. Soc. Rev. 22 (1993) 409–416.
[34] J.F. Fernández-Bertrán, L. Castellanos-Serra, H.Y. Madeira, E. Reguera, J. Solid State Chem. 147 (1999) 561–564.
[35] P.Y. Moh, P. Cubillas, M.W. Anderson, M.P. Attfield, J. Am. Chem. Soc. 133 (2011) 13304–13307.
[36] J. Gregory, Adv. Colloid Interface Sci. 147–148 (2009) 109–123.